Uncovering a Spectrally Hidden REMPI Band of CD_3 by Ion Imaging Spectroscopy of the Products of the Cl + $CHD_3(1_13_1)$ Reaction†

Jens Riedel and Kopin Liu*

Institute of Atomic and Molecular Sciences (IAMS), Academia Sinica, P.O. Box 23-166, Taipei, Taiwan 10617

Received: December 08, 2008; Revised Manuscript Received: December 30, 2008

In the course of studying the reaction dynamics of Cl + $CHD_3(1_13_1) \rightarrow$ HCl + CD_3, an unexpected ring-like feature was observed on the $CD_3(0_0^0)$ product image. By using the technique of ion imaging spectroscopy, the mysterious feature was tentatively ascribed to the formation of the vibrationally excited $CD_3(3_14_1)$ product from the above combination-band excited reaction. The intriguing aspect of the present finding is that the corresponding (2+1)-REMPI band of $CD_3(3_1^14_1^1)$ appears totally hidden by the more intense $CD_3(0_0^0)$ origin band, yet the two-dimensional nature of the ion imaging technique enables us to decipher its spectral character and extract the otherwise lost dynamical information.

I. Introduction

Recent years have witnessed a wide range of applications of ion imaging techniques, using either the original crushed version or a time-sliced velocity-map scheme, for studying chemical dynamics problems.[1−4] In the typical experiment, the energetic of the system and the identity of the probed state are known, thus, the observed image structures reveal the dynamical traits of the probed state by virtue of energy and momentum conservations. In principle, the opposite direction can be taken, in which the image feature is used, with sufficiently high translational energy resolution, to identify the unknown product state or to assign a hitherto unidentified REMPI (resonance-enhanced multiphoton ionization) spectral peak. We have previously exploited that approach to assign, for the first time, the 1_1^1, 3_1^1, and 4_1^1 bands of the (2+1)-REMPI ($3p_z^2A'' \leftarrow\leftarrow \tilde{X}^2A_2''$) transition of CD_3,[5] as well as the 2_1^1, 3_1^1, and 5_1^1 bands of the CHD_2 radical.[6,7] In the latter study, the Extended Cross Correlation analysis was introduced to unravel heavily overlapped multicomponent images.[7] [The conventional notation of 2_1^1 band denotes one-quantum excitation of the vibrational mode number 2 in both the electronical ground state (for the subscript) and the intermediate, two-photon resonant Rydberg state (for the superscript).] We dubbed this approach (ion-) imaging spectroscopy (or spectroscopy by ion imaging).[5]

Imaging spectroscopy is two-dimensional by nature—in terms of the frequency domain of the optical spectrum as well as the ro-vibrational energy level of the neutral species. In all previous applications,[5−7] a distinct, unknown REMPI peak was first observed. We then exploited the velocity-map imaging technique to determine the internal energy excitation, from which the unknown REMPI peak can then be assigned. As will be shown in this report, a totally unexpected situation is encountered, in which *no* new REMPI peak is discernible, yet energetically an unknown excited state must be simultaneously probed to account for the distinct image structure.

The problem occurred in an experiment concerning the reactivity of a combination-band excited $CHD_3(1_13_1)$ with chlorine atom. Recently we reported a series of studies on the relative reactivity of Cl + CHD_3 with one-quantum CH-stretch excitation ($\nu_1 = 1$ or 1_1) and one-quantum excitation of the bending (3_1)/torsional (6_1) modes of CHD_3, respectively.[8−11] The aim of the present study is to explore the synergetic effect, i.e., how does the vibrational enhancement factor for a reaction with combination-band excited CHD_3 compare to those for the two individual fundamental modes of excitation of CHD_3? Figure 1a shows a sketch along the reaction coordinate for breaking the C−H bond, along with a few most relevant vibration states of the CHD_3 reactant and the HCl + CD_3 product pair of this study. We prepared the combination-band excited $CHD_3(1_13_1)$ by an infrared (IR), optical parametric oscillator/amplifier (OPO/OPA) light and detected the CD_3 products using (2+1) REMPI and a time-sliced velocity imaging scheme to interrogate the relative reactivity, the pair-correlated product energy disposal, and the correlated angular distribution. Figure 1b displays two REMPI spectra with IR-on and IR-off, respectively, in the vicinity of the origin band 0_0^0 of CD_3. Both spectra are nearly identical, except the enhanced intensity when the IR laser is turned on, indicating that the reactivity of the excited $CHD_3(1_13_1)$ is greater than $CHD_3(\nu = 0)$ toward Cl atom. That is not surprising, but, as will be shown later, the observed (IR-on) "0_0^0" spectrum of the CD_3 product cannot be entirely due to its origin band.

II. Experimental Approach and IR-Excitation Efficiency

The experimental approach is similar to the one we have used previously;[8−13] only a brief description of relevant points will be given here. A discharged, pulsed beam of a mixture of ~4% Cl_2 in He was used to generate the Cl atom. A set of shaped electrodes[14] was adopted in this work for better discharge stability and longer electrode lifetime. The target beam of CHD_3 was released from a fast-opening EL pulsed valve.[15] Both pulsed beams are doubly skimmed and then cross in a differentially pumped scattering chamber. The reaction product CD_3 was probed by a (2+1) REMPI scheme through the $3p_z^2A \leftarrow\leftarrow \tilde{X}^2A_2''$ transition.[5,16] The UV probe laser, about 8−10 mJ pulse^{-1} near 333 nm, was softly focused by a $f = 50$ cm cylindrical lens. A time-sliced velocity imaging technique[12,13] then mapped the recoils of the state-tagged CD_3^+ ions.

For preparing the combination-band excited reactant $CHD_3(1_13_1)$,[17] an IR OPO/OPA (Laser Vision) near 4002.3 cm^{-1} was tuned to the $1_0^13_0^1$ band, R(1) transition and softly focused

† Part of the "George C. Schatz Festschrift".

* Corresponding author. E-mail: kliu@po.iams.sinica.edu.tw.

10.1021/jp810802g CCC: $40.75
Published on Web 02/05/2009

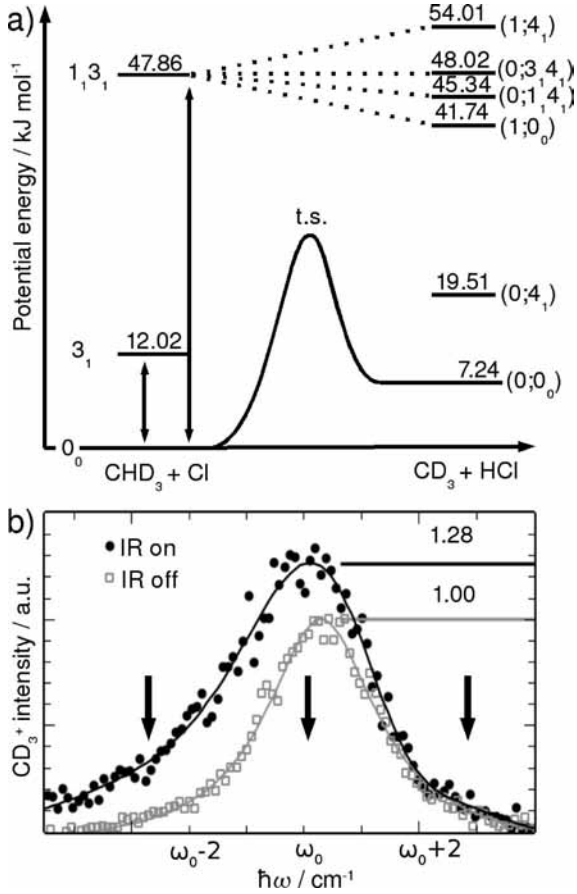

Figure 1. (a) Sketch of the energy profile along the reaction coordinate for producing HCl + CD_3 in the reaction of Cl with CHD_3. The vibrational energy levels of CHD_3 and the HCl + CD_3 product pairs relevant to this study are shown. (b) Two normalized REMPI spectra, IR-on and IR-off, in the vicinity of the Q-head of the $CD_3(0_0^0)$ origin band. The abscissa is the two-photon frequency (in vacuum) with $\omega_0 = 59898.5\ cm^{-1}$.The arrows indicate three probe frequencies at which the representative images are exemplified in Figure 3 for illustration.

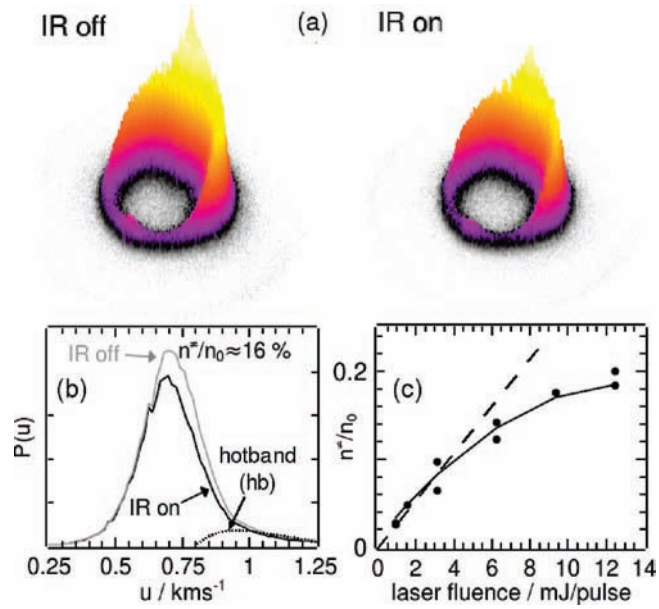

Figure 2. (Color) (a) Raw images of $CD_3(0_0^0)$products, IR-on and IR-off, in the reaction of F + CHD_3 → HF + CD_3. The two images are identical in structure, showing the coincidently formed HF(v=3). The amount of depletion by IR excitation is quantified by the $P(\mu)$ analysis after removing the hot-band contributions from both distributions, shown in panel b. The dependence of IR excitation efficiency or $n^{\neq}/n_0$ on the incident IR laser fluence into the multipass reflector is presented in panel c. The dashed line illustrates the unsaturated, linear absorption behavior. Note that in the usual single-pass configuration, i.e., without the multipass reflector, the estimated excitation efficiency is merely ~2% at the full incident IR fluence.

into a multipass ring reflector[18] just in front of the first skimmer. The photoacoustic spectrum (not shown) of CHD_3 in this region shows complicated patterns comprising the excitation of two combination bands, $\nu_1 + \nu_3$ (band-center at ~3996 cm^{-1}) and $\nu_1 + \nu_6$ (~4029 cm^{-1}).[17] Nevertheless, the dominant spectral features are discernible and a tentative assignment can be made. We found that the R-branch lines of the $1_0^1 3_0^1$ transition (a parallel band) exhibit a distinct doublet −0.40 cm^{-1} splitting. We chose the higher frequency component of the R(1)-doublet for preparing the vibrationally excited $CHD_3(1_1 3_1)$ beam in this experiment.

One of the most crucial quantities in a vibrational excitation experiment of this sort is the fraction of molecules being pumped and contributing to the measured signal, i.e., $n^{\neq}/n_0$. Here $n^{\neq}$ and n_0 denote the number of IR-excited and the initially unexcited molecules (IR-off) in the beam, respectively. Several approaches, including the threshold method,[8] were tried in this study for the determination of $n^{\neq}/n_0$. While all yielded consistent results, the most convenient one turned out to be the depletion experiment using the F + CHD_3 reaction. Figure 2a presents two raw images of $CD_3(0_0^0)$ with IR-on and IR-off, respectively. The two images display identical ring structures with the predominant feature being ascribed, by energy balance, to the coincidently formed HF(v=3) from the ground state reaction. (The weaker structures are too small to be noticed on that scale.)

In other words, when the IR-laser is turned on, no new image feature can be detected and, instead the overall image intensity decreases. The amount of signal decrease can be quantified from the product speed distributions (with the hot-band contribution removed), as demonstrated in Figure 2b. Similar results, i.e., with IR-on image showing smaller signals without any additional feature, were found for the $CHD_2(0_0)$ + DF product channel. We interpreted the observed depletion as the result of IR-excitation that depopulates the ground state reactant $CHD_3(v=0, j=1)$ in the beam. Its dynamical implication is interesting in that the reaction of combination-band excited $CHD_3(1_1 3_1)$ with F-atom apparently does not yield detectable ground state methyl radical products in either isotopic channel. The mode-specific chemistry of that reaction will be reported in the future. Figure 2c summarizes the IR-excitation efficiency (or $n^{\neq}/n_0$) from the depletion measurements as a function of the incident IR fluences. Thanks to the multipass ring reflector that enhances the effective laser fluence by at least 10-fold,[18] the onset of optical saturation is clearly seen even for the present, relatively weak $1_0^1 3_0^1$ transition.

III. A Mysterious Ring-like Structure on Ion Images

Once the IR excitation of the CHD_3 beam was optimized and the pumping efficiency quantified, we switched the radical beam from F- to Cl-atom. Figure 3 shows six raw images of the CD_3 products probed at three wavelengths over the Q-head of the 0_0^0 band. The IR-off images exhibit two adjacent backward/sideways scattered features. On energetic grounds, both features are assigned to the HCl(v=0) + $CD_3(0_0)$ product pairs, with the predominant one from the ground state reaction and the weaker outer-ring from the reaction of Cl with the bend/torsion-excited CHD_3 in the supersonic beam.[19,20]

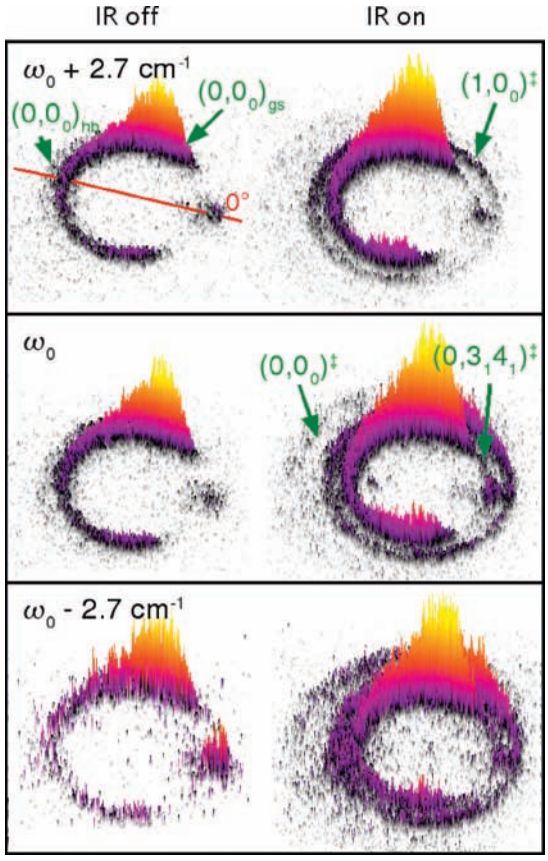

Figure 3. Six raw images of the CD_3 products from the Cl + CHD_3 reaction, probed at three different wavelengths over the Q-head of the 0_0^0 band, are exemplified. On energetic grounds, the product state pairs are identified as indicated. See the text for the notations. Some beam backgrounds along the forward direction are seen, but discarded in data analysis.

The IR-on images display several new features. The outermost feature with the fastest recoil speed clearly corresponds to the Cl + $CHD_3(1_13_1)$ → HCl(v=0) + $CD_3(0_0)$ reaction, denoted as the $(0, 0_0)^{\neq}$ product pair. [The first number in the parentheses gives the vibrational quantum number of the concomitantly formed HCl, and the second number is for the probed CD_3 vibration state. The superscript " ≠ " indicates the product pair formed in the combination-band excited reaction Cl + $CHD_3(1_13_1)$.] Its angular distribution is backward dominant. By conservation of energy, the middle ring is ascribed to Cl + $CHD_3(1_13_1)$ → HCl(v=1) + $CD_3(0_0)$, which is nearly degenerate to the IR-off reaction of Cl + $CHD_3(3_1$ and/or $6_1)$ → HCl(v=0) + $CD_3(0_0)$. We denoted this new feature as $(1, 0_0)^{\neq}$, which is most vividly seen in the forward hemisphere. Because the IR laser should exert no effect on the initially bend/torsion-excited CHD_3 in the beam, the angular distribution of the $(1, 0_0)^{\neq}$ pair can be obtained by simple subtraction of the two normalized IR-on and IR-off distributions, as exemplified in Figure 4 for the images acquired at ω_0 (the middle two of Figure 3). Its angular distribution is characterized by a paramount forward peak superimposed on a broad and nearly isotropic component, in sharp contrast to the $(0, 0_0)^{\neq}$ pair.

As to the innermost ring, which is in complete overlap with the most intense feature on the IR-off image, a new forward component is clearly discernible. Its origin is, however, puzzling and is the focus of the present study. Before discussing the product-pair assignment of this new image feature, we noted that the mysterious forward component appears only when the IR laser was turned on and energetically it nearly coincides with the feature from the HCl(v=0) + $CD_3(0_0)$ product pair in the ground state reaction. [The translational energy resolution of our crossed-beam ion-imaging setup is mostly limited by the initial collision energy spread, which is about 2 kJ mol^{-1} in this study. However, whether the image features can be resolved will also depend on the product rotational state distributions.] To retrieve the angular distribution of this mysterious product pair, we scaled down the IR-off angular distribution by 0.16 (to account for the reduction of the ground state CHD_3 reactants as the IR laser was turned on) and subtracted it from the IR-on data.[8] The genuine distribution for the mysterious pair was then recovered from the overlapped inner ring, as illustrated in Figure 4. Despite the larger uncertainty due to the small differences between two large numbers, the angular distribution shows a pronounced forward peak and a broad sideway/backward scattered component.

IV. Assignments of the Mysterious Image Feature and the Hidden REMPI Band

When acquiring the images, the probe laser frequencies were fixed in the vicinity of the Q-head of the $CD_3(0_0^0)$ band, which are spectroscopically distinct from any other known vibronic bands such as 1_1^1, 2_1^1, 3_1^1, 4_1^1 etc.[5] Hence, one would have thought that only the ground vibrational state $CD_3(0_0)$ was probed. At E_c = 21.6 kJ mol^{-1}, two states, v = 0 and 1, of HCl coproducts are energetically accessible and their appearances on the image have already been identified as discussed above. Then, what could be the origin of the mysterious image feature? This leaves us with only two possibilities: as either the rotationally hot HCl or some vibrationally excited state of CD_3 whose REMPI transition, hitherto unobserved, just happens to overlap with the 0_0^0 origin band.

The first possibility will lead to a bimodal rotation distribution of HCl concomitantly formed with the probed $CD_3(0_0)$ products. Judging from the fact that the two (inner) image features are so well-resolved and with the corresponding energy difference approaching 12 kJ mol^{-1}, such a sharply peaked bimodal rotation distribution seems odd. Alternatively, it will be ascribed to a vibrationally excited CD_3 product with a nearly identical kinetic energy release (as evident from the observed images) to the HCl(v=0) + $CD_3(0_0)$ product pair in the ground state reaction. As depicted in Figure 1a, three product pairs with vibrationally excited CD_3, (1, 4_1), (0, 3_14_1), and (0, 1_14_1), are the plausible candidates. [The vibrational mode conventions for CD_3 radical are ν_1 for the symmetric stretch, ν_3 for the antisymmetric stretch, and ν_4 for the in-plane bend.] Energetically, the $(1, 4_1)^{\neq}$ pair is endothermic by 6.14 kJ mol^{-1} with respect to the Cl + $CHD_3(1_13_1)$ reactants, which is the closest to the endothermicity (7.24 kJ mol^{-1}) for the ground state reaction of Cl + CHD_3 → HCl(v=0) + $CD_3(0_0)$. Spectroscopically,[5] the $CD_3(4_1^1)$ band is known to blue-shift from the 0_0^0 band by 22 cm^{-1}—too far to be the case. Thus, we excluded the (1, 4_1) pair. The other two pairs involve the combination-band excited CD_3. The heats of reaction from the Cl + $CHD_3(1_13_1)$ reactants are endothermic by 0.16 kJ mol^{-1} for forming the (0, 3_14_1) product pair and exothermic by −2.52 kJ mol^{-1} for (0, 1_14_1). On the basis of the fundamental vibration frequencies of the $\tilde{X}^2A_2''$ and $3p_z^2A''$ states,[5] the corresponding REMPI bands are estimated to red-shift from the 0_0^0 band by −30 and −13 cm^{-1} for the $1_1^14_1^1$ and $3_1^14_1^1$ transitions, respectively. The actual band positions will be somewhat different when the (unknown) anharmonicities are taken into account. In addition, both the ν_3 and ν_4 modes are of e-type symmetry, so that one-quantum excitation of the combination band of ν_3 and ν_4 modes in both

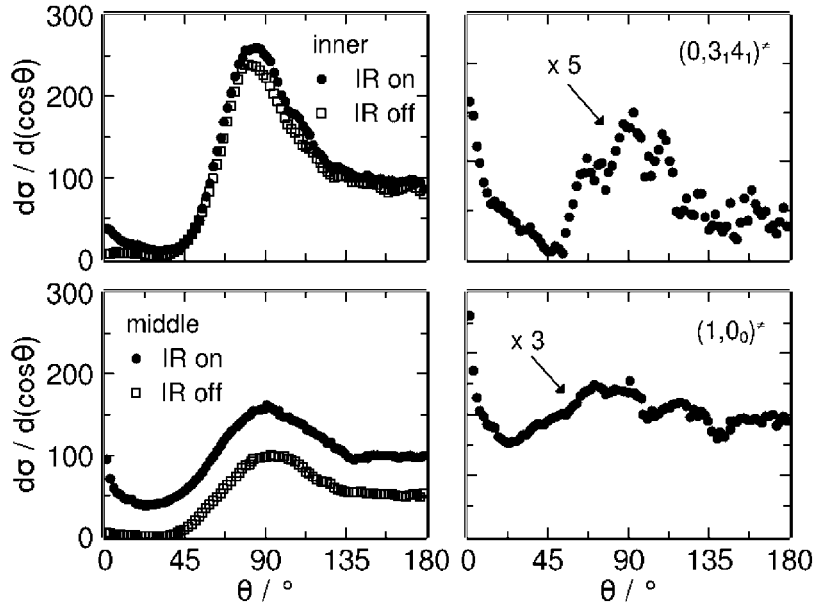

Figure 4. Product angular distributions for the two overlapped ring-like features are illustrated for the probe laser frequencies fixed at ω_0. The distributions shown in the left panels are for IR-on (the solid circle) and IR-off (the open square). The derived genuine distributions for the $(1,0_0)^{\neq}$ and $(0,3_14_1)^{\neq}$ product pairs are presented in the upper-right and the lower-right panels, respectively. See the text for the details.

the electronical ground and the excited states will consist of three levels, a_1, a_2, and e symmetry, which will likely be split in energy by different amounts in the two electronic states. As a result, the $3_1^1 4_1^1$ REMPI transition may comprise at least three bands. It would not be at all surprising if one (or more) of them accidently happens to overlap with the origin band. Hence, although the possibility of $1_1^1 4_1^1$ could not be completely ruled out, tentatively we favor the assignment to the $3_1^1 4_1^1$ band.

As a self-consistent check of all product-pair assignments and the angular analysis of the IR-on image, we next examined the product speed distributions. Presented in Figure 5 are the three $I(\mu)$ distributions of the probed CD_3 products deduced from the images shown in Figure 3. Note that the conventional product speed distribution $P(\mu)$ is defined as $d\sigma/d\mu$.[21] Since the additional image features from the combination-band excited reaction are most readily seen in the forward direction, they usually make small contributions to total reactive flux due to the smaller solid-angle factors. To have a more faithful view of their contributions to the sliced image (in number density), we plot in Figure 5 the speed distribution defined as $I(\mu) \equiv P(\mu)/\sin\theta$. Also depicted in the figure is the individual contribution from each of the assigned product pairs. This partitioning procedure was performed in the following way. For each component the angle-integrated intensity was taken from the angular distribution (Figure 4, without the $\sin\theta$-weighting factor) and its speed limit was bound by the conservation of energy. In addition, to minimize the number of free parameters in partitions, the IR-off $I(\mu)$ was fitted first and then inserted directly (with proper scaling factors) into the IR-on $I(\mu)$ distribution. The black line gives the sum of such a partitioning, which is in excellent agreement with the actual experimental data (the open circles).

We now look back at the REMPI spectra, trying to uncover the composition or the spectral signature of each component. Over the 0_0^0 Q-head, ten pairs of IR-on and IR-off images were acquired at different wavelengths. Note that the REMPI signal reflects the product density, whereas the analyzed result from the ion image represents the reactive flux into each of the product pairs.[12,13] Hence, from the analyzed images, we retrieved the corresponding REMPI signal for each partitioned flux

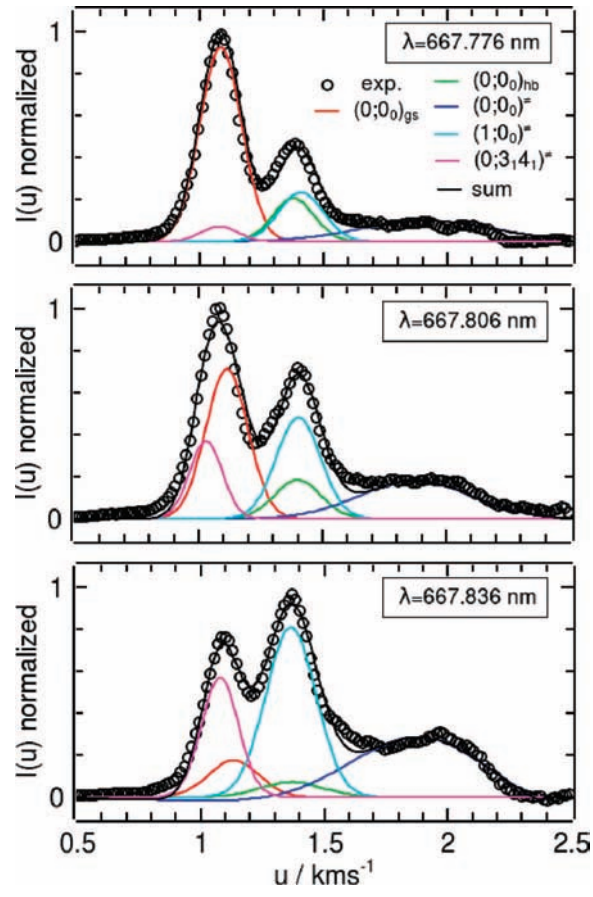

Figure 5. Three $I(\mu)$ distributions of the CD_3 products deduced from the three images shown in Figure 3 are presented. Note that the $I(\mu)$ is not the conventional product speed distribution, rather defined as $I(\mu) = (d\sigma/d\mu)/\sin\theta$. Also shown are the contributions from each of the assigned product pairs. The black line denotes the sum of such a partitioning and the actual experimental data points are given as the open circles.

component. The results are summarized in Figure 6 for the IR-on spectrum. Also marked on top of the figure are the spectral locations of the rotational transitions of the CD_3 (0_0^0) band. As

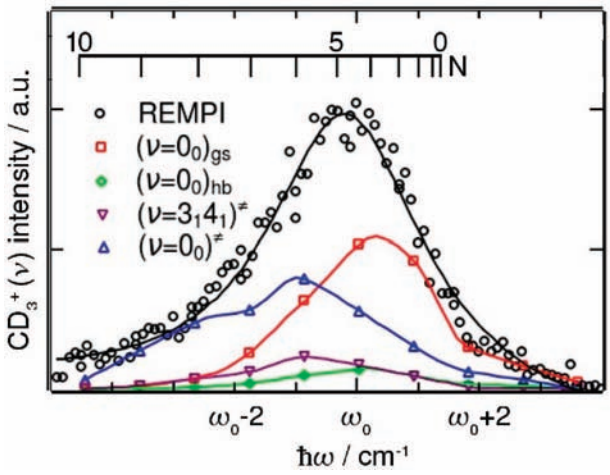

Figure 6. Partitioning of the IR-on REMPI spectrum of the CD_3 products from various product-pair channels in the Cl + CHD_3 reaction.

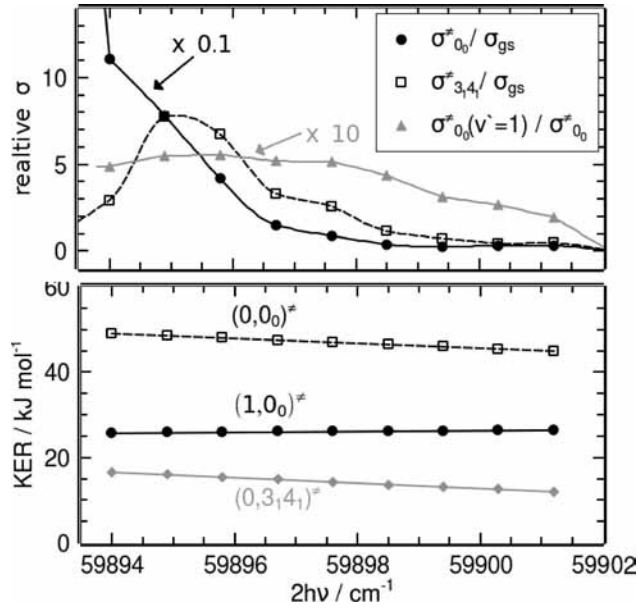

Figure 7. Top panel: Dependence of the relative cross sections on the probe laser frequencies over the $CD_3(0_0^0)$ origin band. Bottom panel: Kinetic energy release (KER) of the indicated product state pairs as a function of the probe laser frequencies, showing their dependence on the probed $CD_3(\nu=0, N)$ states for the $(0,0_0)^{\neq}$ and $(1,0_0)^{\neq}$ product pairs. Note that the red shift corresponds to higher N states of $CD_3(0_0)$.

is seen, both the ground state (gs) and bend-excited (hb) reactions, labeled as $(\nu = 0_0)_{gs}$ and $(\nu = 0_0)_{hb}$, produce similar rotational contours, peaking around $N \approx 3-4$. The vibrational ground state product $CD_3(0_0)$ from the combination-band excited reaction, $(\nu = 0)^{\neq}$, yields slightly warmer rotation distribution, peaking around $N \approx 6$. Interestingly, a similar spectral profile is found for the combination-band excited product $(\nu = 3_14_1)^{\neq}$. Consequently, the IR-on REMPI spectrum appears more red-shaded than the IR-off, as seen in Figure 1.

V. Implications to Reaction Dynamics

As mentioned in the Introduction, the objective of this project is to explore the mode-specific chemistry, in particular the synergetic effect of combination-band excited $CHD_3(1_13_1)$ reactivity when compared to the excitation of the individual fundamental mode, $CHD_3(1_1)$ and $CHD_3(3_1)$; in other words, will the relative reactivity be more enhanced or somewhat prohibited? It is appropriate at this point to make a scrutiny into the dynamical aspects of our findings.

First, as already noted, the $CD_3(0_0)$ products from the combination-band excited reaction show slightly more rotational excitation than the $CD_3(0_0)$ products from either the ground state or the bend-excited reaction. Although the rotational analysis cannot be made for the combination-band excited $CD_3(3_14_1)$ products, it appears that the rotational energy disposals of CD_3 products in all cases are rather small.

Second, we examined the state-correlation of the product pairs. For the ground state reaction Cl + $CHD_3(0_0) \rightarrow$ HCl(ν=0, j) + $CD_3(0_0, N)$, the general trend is that as N increases, j decreases. This *negative* correlation between N and j can be seen from Figure 5: as the probe laser frequency red-shifts (i.e., toward higher N), the average speed of the $(0, 0_0)_{gs}$ component becomes faster (i.e., more kinetic energy release), resulting in lower j-excitation. For the HCl(ν) + $CD_3(0_0, N)$ product pair from the combination-band excited reaction Cl + $CHD_3(1_13_1)$, a *positive* correlation of the more $\nu = 1$ of HCl for the higher N was found, as demonstrated in the upper panel of Figure 7. By way of contrast, previously we found a *negative* correlation between the HCl vibrational excitation ($\nu = 1$) and the rotational excitation N of the $CD_3(0_0)$ for the Cl + $CHD_3(1_1) \rightarrow$ HCl(ν) + $CD_3(0_0, N)$ reaction.[9]

Also summarized in the lower panel of Figure 7 are the kinetic energy releases (KER) of the three vibrational product pairs. While the KER for the $(1, 0_0)^{\neq}$ pair is nearly invariant to the selected CD_3 N-states, that for the $(0, 0_0)^{\neq}$ clearly indicates a larger KER for the higher N-states. In other words, as the $CD_3(0_0)$ product is formed with higher rotational excitation, both the average KER and the correlated vibrational excitation of the HCl coproducts increase. By virtue of energy conservation, the corresponding rotational excitation of HCl, in particular HCl(ν=0), must then be less, i.e., an anticorrelation between N and j of the two product rotors—a trend similar to the aforementioned ground state reaction. Unfortunately the rotational contour of the $3^1_14^1_1$ REMPI band is not known, rendering the similar $N-j$ correlation analysis for the Cl + $CHD_3(1_13_1) \rightarrow$ HCl(ν=0, j) + $CD_3(3_14_1, N)$ channel difficult. Nevertheless, the average HCl rotational energy in this channel appears to be larger than the other paired channels. On the basis of the average HCl rotational energy (deduced from the peak of the P(μ) distribution and the energetic limit), at ω_0 the average $\langle j\rangle_{HCl}$ correlated to $CD_3(\nu$=0) from both the ground state and combination-band excited reactions are about 3−4, and that correlated to $CD_3(3_14_1)$ from the Cl + $CHD_3(1_13_1)$ reaction is significantly larger, $\langle j\rangle_{HCl} \sim 8$. It is worth noting that the combination-band excited CHD_3 reactant involves one-quantum excitation each in the C−H stretching (ν_1) and the CD_3 umbrella bending (ν_3) modes, thus both motions retain the $C_{3\nu}$ symmetry configuration. If the transition state geometry favors a collinear Cl−H−C configuration as suggested by ab initio calculations,[22−25] then the reactive trajectories leading to the combination-band excited product $CD_3(3_14_1)$, which involves the antisymmetric stretching (ν_3) and the deformed (in-plane) bending (ν_4) motions of CD_3, must break the $C_{3\nu}$ symmetry of the minimum energy path, thus experiencing significant anisotropic interactions that could conceivably exert larger torques to the two departing product rotors. Further investigation into this intriguing finding is in progress.

Finally, Table 1 summarizes the relative cross sections for reactions with the vibrationally excited and ground state CHD_3 reactants. Since the relative cross sections exhibit clear dependence on the probed N-states (Figure 7), the results for both ω_0

TABLE 1: Comparison of the Vibrational Enhancement Factors of Three Different Modes of Excitation of CHD_3: $\sigma^{\neq}_{0_0}/\sigma_{gs}$ for Cl + $CHD_3(1_13_1) \rightarrow HCl(v) + CD_3(0_0)$, $\sigma^{\neq}_{3_14_1}/\sigma_{gs}$ for Cl + $CHD_3(1_13_1) \rightarrow HCl(v=0) + CD_3(3_14_1)$, $\sigma^{\neq}(1_1)/\sigma_{gs}$ for Cl + $CHD_3(1_1) \rightarrow HCl(v) + CD_3(0_0)$, and $\sigma^{\neq}(3_1/6_1)$ for Cl + $CHD_3(3_1/6_1) \rightarrow HCl(v=0) + CD_3(0_0)$[a]

λ_{probe}	$\sigma^{\neq}_{0_0}$	$\sigma^{\neq}_{3_14_1}/\sigma_{gs}$	$(\sigma^{\neq}_1/\sigma^{\neq})_{0_0}$	$\sigma^{\neq}(1_1)\sigma_{gs}$	$\sigma^{\neq}(3_1/6_1)/\sigma_{gs}$
peak (ω_0)	3.7	1.1	0.44	4.5	2.5
band integrated	6.5	1.5	0.47		

[a] The latter two are taken from ref 10. The correlated HCl vibrational branching fraction defined as $HCl^{\neq}(v=1)/[HCl(v=1) + HCl(v=0)]^{\neq}$, i.e., $(\sigma_1^{\neq}/\sigma^{\neq})_{0_0}$, refers to the first reaction. All entries are at $E_c = 21.6$ kJ mol^{-1}, and σ_{gs} is the cross section of the ground state reaction.

(near the peak of REMPI spectrum) and the integrated one (over the REMPI band) are listed for comparison. Compared to the ground state reaction cross section σ_{gs}, the reactive cross sections for forming the $CD_3(0_0)$ and $CD_3(3_14_1)$ products from the combination-band excited reactant, i.e., $\sigma^{\neq}_{0_0}$ and $\sigma^{\neq}_{3_14_1}$, respectively, are 3.7 and 1.1 times larger when the probe-laser frequency is fixed near the REMPI peak. [Note that the relative sensitivities of REMPI detection of the $CD_3(0_0)$ and $CD_3(3_14_1)$ states are yet to be calibrated.] When integrating over the "0^0_0" REMPI band, vibrational enhancement factors for both product channels increase to 6.5 and 1.5, respectively. The HCl vibrational branching fraction correlated to the $CD_3(0_0)$ products, $(\sigma_1^{\neq}/\sigma^{\neq})_{0_0}$, also increases slightly from 0.44 to 0.47 by the two measures, which is to be compared to the values (for the probe laser at ω_0) of 0.44 and ~0 in the Cl + $CHD_3(1_1)$ and Cl + $CHD_3(3_1)$ reactions, respectively.[10] The previous report on the vibrational enhancement factors for both the stretch-excited and bend-excited CHD_3 reactions are for probe wavelength fixed at the peak of the 0^0_0-REMPI band, and the results are about 4.5 and 2.5 at $E_c = 21.6$ kJ/mol for $\sigma^{\neq}_{1_1}$ and $\sigma^{\neq}_{3_1}/\sigma_{gs}$, respectively.[10] In other words, the vibrational enhancement factor for the 1_13_1 combination-band excitation does not appear to be much different from the pure stretch- or bend-excited reactions, implying no significant synergetic effect. Of course, many other vibrationally excited products remain to be interrogated; preliminary study, however, indicated that the states probed in this work account for the majority of reactive fluxes. The present finding then suggests that the mode-specific reactivity of a combination-band excited reactant could be more complicated and does not appear to have a simple relationship to the reactivity of the individual mode of excitation, as one might have intuitively thought (or hoped for). By way of contrast, previous study of the Cl + $CD_4(\nu_4) \rightarrow DCl(v=0) + CD_3(0_0)$ reaction demonstrated a simple relationship for overtone-excitation of the bending mode of CD_4: $\sigma(\nu_4=2)/\sigma(\nu_4=1) \approx \sigma(\nu_4=1)/\sigma(\nu_4=0) \approx 3$.[20] We note that the normal-mode assignment is only an approximate, zeroth-order picture of the vibrational motion. Although the present C−H stretching mode (1_1) and the CD_3-bending mode (3_1) appear to provide a reasonable description of the nuclear motions,[17] the amplitude of the 1_13_1 combination band invokes the coherent motions of the two fundamental modes. On the other hand, the bend-excited CD_4, either $\nu_4 = 1$ or 2, is of the same umbrella movement with different amplitudes. Will the observed different synergetic behaviors for the combination-band and the overtone excitations be a manifestation of the different phase relationship of the fundamental mode amplitudes? Further works, both experimental and theoretical, are needed for deeper insights.

Acknowledgment. We gratefully acknowledge S. Yan for the tentative assignment of the combination band of CHD_3 photoacoustic spectra and Y. T. Wu for his help in acquiring some of the data. This work was financially supported by the National Science Council of Taiwan, Academia Sinica, and the US Air Force Office of Scientific Research (AOARD-07-4005).

References and Notes

(1) Heck, A. J. R.; Chandler, D. W. *Annu. Rev. Phys. Chem.* **1995**, *46*, 335.
(2) Townsend, D.; Li, W.; Lee, S. K.; Gross, R. L.; Suits, A. G. *J. Phys. Chem. A* **2005**, *109*, 8661.
(3) Ashfold, M. N. R.; Nahler, N. H.; Orr-Ewing, A. J.; Vieuxmaire, O. P. J.; Toomes, R. L.; Kitsopoulos, T. N.; Garcia, I. A.; Chestakov, D. A.; Wu, S.-M.; Parker, D. H. *Phys. Chem. Chem. Phys.* **2006**, *8*, 26.
(4) Liu, K. *Phys. Chem. Chem. Phys.* **2007**, *9*, 17.
(5) Zhang, B.; Zhang, J.; Liu, K. *J. Chem. Phys.* **2005**, *122*, 104310.
(6) Zhou, J.; Lin, J. J.; Liu, K. *J. Chem. Phys.* **2003**, *119*, 8289.
(7) Zhang, B.; Yan, S.; Liu, K. *J. Phys. Chem. A* **2007**, *111*, 9263.
(8) Yan, S.; Wu, Y.-T.; Liu, K. *Phys. Chem. Chem. Phys.* **2007**, *9*, 250.
(9) Yan, S.; Liu, K. *Chin. J. Chem. Phys.* **2007**, *20*, 333.
(10) Yan, S.; Wu, Y.-T.; Zhang, B.; Yue, X.-F.; Liu, K. *Science* **2007**, *316*, 1723.
(11) Yan, S.; Wu, Y.-T.; Liu, K. *Proc. Natl. Acad. Sci. U.S.A.* **2008**, *105*, 12667.
(12) Lin, J. J.; Zhou, J.; Shiu, W.; Liu, K. *Rev. Sci. Instrum.* **2003**, *74*, 2495.
(13) Lin, J. J.; Zhou, J.; Shiu, W.; Liu, K. *Chin. J. Chem. Phys.* **2004**, *17*, 346.
(14) Lu, I.-C.; Huang, W.-J.; Chaudhuri, C.; Chen, W.-K.; Lee, S.-H. *Rev. Sci. Instrum.* **2007**, *78*, 083103.
(15) Even, U.; Jortner, J.; Noy, D.; Lavie, N. *J. Chem. Phys.* **2000**, *112*, 8068.
(16) Hudgens, J. M.; DiGiuseppe, T. G.; Lin, M. C. *J. Chem. Phys.* **1983**, *79*, 571.
(17) Carter, S.; Shnider, H. M.; Bowman, J. M. *J. Chem. Phys.* **1999**, *110*, 8417.
(18) Riedel, J.; Yan, S.; Kawamata, H.; Liu, K. *Rev. Sci. Instrum.* **2008**, *79*, 033105.
(19) Zhou, J.; Zhang, B.; Lin, J. J.; Liu, K. *Mol. Phys.* **2005**, *103*, 1757.
(20) Zhou, J.; Lin, J. J.; Zhang, B.; Liu, K. *J. Phys. Chem. A* **2004**, *108*, 7832.
(21) Levine, R. D.; Bernstein, R. B. *Molecular Reaction Dynamics and Chemical Reactivity*; Oxford University Press: New York, 1987.
(22) Duncan, W. T.; Truong, T. N. *J. Chem. Phys.* **1995**, *103*, 9642.
(23) Corchado, J. C.; Truhlar, D. G.; Espinosa-Garcia, J. *J. Chem. Phys.* **2000**, *112*, 9375.
(24) Troya, D.; Weiss, P. J. E. *J. Chem. Phys.* **2006**, *124*, 074313.
(25) Castillo, J. F.; Aoiz, F. J.; Banares, L. *J. Chem. Phys.* **2006**, *125*, 124316.

JP810802G